Limnol. Oceanogr., 52(5), 2007, 1809–1823

Biogeochemical composition of natural sea ice brines from the Weddell Sea during early austral summer

S. Papadimitriou,[1] *D. N. Thomas and H. Kennedy*
Ocean Sciences, College of Natural Sciences, University of Wales–Bangor, Menai Bridge, Anglesey LL59 5AB, United Kingdom

C. Haas
Alfred Wegener Institute for Polar and Marine Research, Am Hadelshafen 12, D-27570 Bremerhaven, Germany

H. Kuosa
Tvärminne Zoological Station, University of Helsinki, FI-109100 Hanko, Finland

A. Krell and G. S. Dieckmann
Alfred Wegener Institute for Polar and Marine Research, Am Hadelshafen 12, D-27570 Bremerhaven, Germany

Abstract

Sea ice brines were collected from a single floe composed of different ice types in the western Weddell Sea in December 2004. The chemical composition of the brines (temperature: −3.4°C to −2.1°C; salinity: 40–63) was examined on seven occasions over 25 days with measurements of dissolved oxygen, dissolved inorganic macronutrients (nitrate plus nitrite, ammonium, phosphorus [DIP], and silicic acid), pH, total alkalinity (A_T), dissolved organic carbon (DOC) and nitrogen (DON), total dissolved inorganic carbon (C_T), and the stable isotopic composition of C_T ($\delta^{13}C_T$). The in situ pH ranged from 8.41–8.82 on the seawater scale, dissolved oxygen from 212–604 μmol kg^{-1}, nitrate from 0.1–3.1 μmol kg^{-1}, ammonium 0.1–2.4 μmol kg^{-1}, DIP 0.4–2.0 μmol kg^{-1}, silicic acid 4–80 μmol kg^{-1}, A_T 2,690–4,620 μeq kg^{-1}, DOC 115–359 μmol kg^{-1}, DON 8–26 μmol kg^{-1}, C_T 2,090–3,550 μmol kg^{-1}, and $\delta^{13}C_T$ +2.9‰–+6.4‰. Compared with the chemical composition of surface oceanic water (salinity of 34), the brines had elevated pH, reduced concentrations of dissolved inorganic macronutrients (including carbon), especially dissolved inorganic nitrogen, and were mostly supersaturated with dissolved oxygen with respect to equilibrium with air, whereas the C_T was considerably enriched in ^{13}C. The chemical composition of the brines was consistent with internal biological productivity, but there was a lack of a distinctive and uniform relationship among the major dissolved inorganic nutrients typically used for describing biological activity. This was interpreted as the result of varying stoichiometry of biological activity within a very small spatial scale. Modification by abiotic processes was a potential contributing factor, such as degassing acting on the dissolved oxygen concentration. Carbonate mineral formation, acting on A_T and C_T, was not evident in brines from first-year ice but was apparent in brine from second-year ice.

Sea ice covers 13% of the surface of the earth at its maximum extent, equivalent to the areal extent of deserts and tundra. The largest expanse of sea ice occurs in the Southern Ocean, totalling 18.8 × 10^{16} km^2 of 0.5–0.6 m mean thickness at its maximum extent in September (Comiso 2003). It is an ecologically diverse habitat and has been increasingly recognized for its key role in global biogeochemical cycles, including contribution to the primary productivity of the Southern Ocean (Arrigo 2003; Arrigo and Thomas 2004) and the ventilation of the deep ocean at high latitudes (Francois et al. 1997; Stephens and Keeling 2000).

The chemical composition of sea ice is primarily a function of salinity and temperature, but it is modified further by productivity of the internal microbial assemblages recruited from the surface seawater during sea ice formation (Brierley and Thomas 2002; Thomas and Dieckmann 2002; Rysgaard et al. 2007). Primary production is a major carbon sink within sea ice, resulting in the fixation of 30–70 Tg C yr^{-1} into biomass in the first- and multi-year ice pack of the Southern Ocean (Arrigo and Thomas 2004). The effect of primary production was evident in the chemical composition of sea ice brines extracted from several locations in the Weddell Sea in austral summer and autumn as an accumulation of

[1] Corresponding author (s.papadimitriou@bangor.ac.uk).

Acknowledgments

We thank the master and crew of the RV *Polarstern* for their help in making this sampling possible, as well as colleagues from the Ice Station Polarstern (ISPOL) team who helped in fieldwork activities. Support with preparation for the expedition and subsequent analyses was given by Marcel Nicolaus, Anja Batzke, Paul Kennedy, Louiza Norman, Hannah Betts, Erika Allhusen, and Rachel Thomas. We are grateful to G. M. Marion for providing the code of the FORTRAN version of the Spencer-Moller-Weare chemical thermodynamic model for aqueous electrolyte solutions at sub-zero temperatures (FREZCHEM, Version 8.2). We also thank W. H. Jeffrey and two anonymous reviewers for their constructive comments.

This project was supported by the UK Natural Environmental Research Council (NERC), The Leverhulme Trust, and The Royal Society.

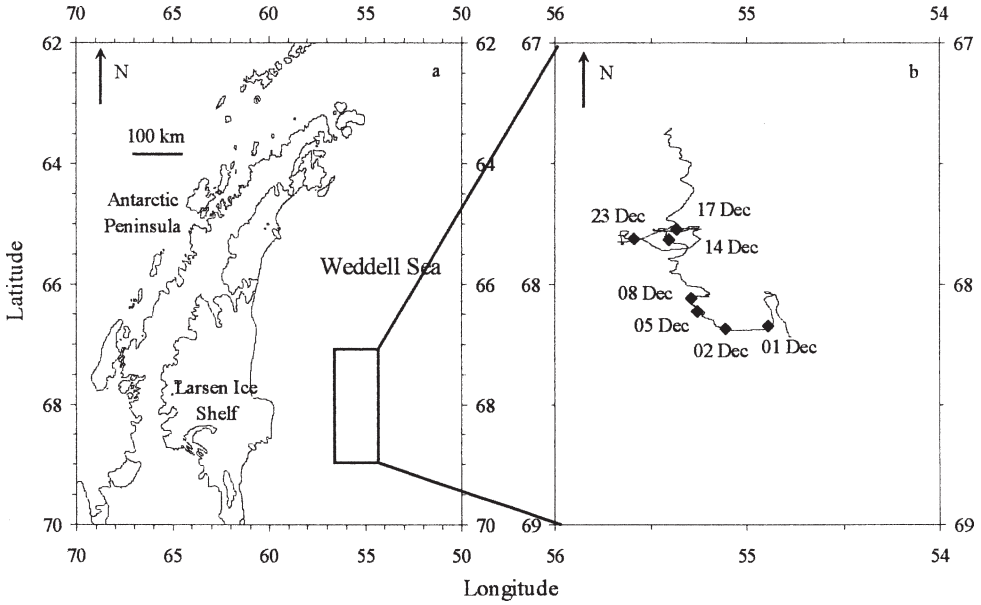

Fig. 1. (a) Location of the ISPOL drift in the western Weddell Sea shown by the square, and (b) the drift track annotated with the sackhole sampling dates.

dissolved oxygen (O_2), the pH rise from 8 to 10, and the drawdown of the major dissolved inorganic nutrients (Gleitz and Thomas 1993; Gleitz et al. 1995). Further compositional changes commensurate with biological activity have been derived from ice-water interfacial habitats (i.e., gap waters and bottom sea ice communities) in austral spring (Arrigo et al. 1995), summer (Kennedy et al. 2002; Kattner et al. 2004), and mid-autumn (Gleitz and Thomas 1993).

Because of the strong compositional modification of natural sea ice brines by biological activity, little attention has been paid to any potential contribution by abiotic processes, such as gas exchange and mineral formation. The freezing of seawater results in the expulsion of the dissolved salts from the ice crystal matrix, leading to increased ionic strength of the residual liquid (brine) trapped within sea ice (Eicken 2003). The rise in salinity in combination with the subzero temperatures in the ice sheet induce changes in the mineral–liquid and gas–liquid thermodynamic equilibria within sea ice, leading to degassing and mineral precipitation from the highly concentrated brine (Killawee et al. 1998; Marion 2001; Papadimitriou et al. 2004). In the most thermodynamically consistent sequence of minerals precipitating from brines at sub-zero temperatures and 1 atm, carbonate mineral ($CaCO_3$) formation is predicted to occur first at $-2.2^{\circ}C$, followed by a suite of mineral phases (sodium and calcium sulfate, as well as sodium, potassium, and magnesium chloride) at progressively lower temperatures (Marion and Farren 1999; Tison et al. 2002; Eicken 2003). The precipitation of $CaCO_3$ from brine represents an additional potential carbon sink within sea ice along with internal primary production, the dynamics of which are largely unknown in natural settings.

Sea ice is a field of investigation with limited accessibility and considerable spatial and temporal heterogeneity in both the horizontal and vertical extent of its physical–chemical characteristics. The existing evidence regarding controls on the biogeochemical composition of sea ice is still sparse in space and time by comparison with other major biomes on earth. This study describes the composition of natural sea ice with respect to biologically important solutes (nutrients) and dissolved gases (O_2 and carbon dioxide [CO_2(aq)]) in early austral summer. The aim was to characterize extensively the environment experienced by the internal microbial assemblages of sea ice in the transition from spring to summer with the minimal sample manipulation achieved by in situ brine collection as opposed to melted or centrifuged bulk ice. The study was conducted on a single ice floe, which offered greater constraint on horizontal spatial variability than previously achieved with a similar sampling protocol in Gleitz et al. (1995). The current results include the first direct measurements of the dissolved inorganic carbon pool and its stable isotopic composition in natural sea ice brines.

Study site and sampling

The sampling took place on a 10 km × 10 km (initial dimensions) ice floe in the western Weddell Sea during the field experiment Ice Station Polarstern (ISPOL; www.ispol.de) onboard the German research icebreaker *Polarstern* in December 2004 at approximately 67–68°S and 55° W (Fig. 1). At the end of the field experiment (02 January 2005), the floe was approximately 120 nautical miles (222 km) from the marginal ice zone (ice edge). Satellite radar imagery indicated that the ISPOL floe was located at the boundary between a region with predominantly second-year ice from the central Weddell Sea in the east and a region of first-year ice in the west (Hellmer et al. 2006). The latter originated from a recurring polynya off the Filchner-Ronne Ice Shelf approximately 1,000 km south of

the study region, where it was formed in March or April 2004, i.e., 8 to 9 months before sampling. The ISPOL floe consisted mainly of 200–250-cm-thick second-year ice covered by approximately 80 cm of snow, small patches of 80-cm-thick first-year ice formed locally, and large fragments of 150–180-cm-thick first-year ice from the Filchner-Ronne polynya with a 30-cm snow cover (Hellmer et al. 2006). Only little snow thinning was observed during the course of the study (op. cit.). All measurements described here were obtained from bulk ice and brine between days 336 (01 December) and 353 (18 December) of the year from an approximately 50 m × 50 m patch of level thick first-year ice, except for one occasion on day 358 (23 December 2004) when brine from second-year ice was sampled.

Brine samples were collected on seven occasions using the sackhole sampling technique in which brine is allowed to percolate into partial core holes in the ice surface (Gleitz et al. 1995). On each occasion, the snow cover was removed manually from within a 1 m^2 surface area, and two to ten sackholes were cored with a stainless steel ice corer (Kovacs, 10 cm internal diameter) either by hand or powered by an electric motor with the generator sited 5 m from the coring site. The sampled patches were approximately 20 m apart from each other. Typically, sufficient brine volume was collected in 5–10 minutes in a covered core hole of 10-cm diameter and 20–60 cm depth. With minimal wind velocity over the surface of the liquid brine collecting in the covered core hole, the air-brine diffusive boundary layer is expected to be maximal, on the order of 500–1,000 μm (Emerson 1975). In these sheltered conditions, non-chemically enhanced, diffusive gas exchange with the atmosphere across the diffusive boundary layer at -2°C to -3°C in situ brine temperature was calculated to be minimal for the measured concentrations of O_2 and CO_2(aq), using the equation in Emerson (1975) for appropriate diffusion coefficients and air equilibrium concentrations. Sackhole sampling is adequate for measurements of dissolved constituents in brines, but has been shown to be unsuitable for quantitatively estimating the particulate fraction (Weissenberger 1992). Therefore, the information about organisms we present here offers only an approximate description of the composition of the biological community in the ice sampled.

Companion ice cores for measurements of bulk ice properties were taken on four occasions with an electrically powered stainless steel ice corer as described earlier. The cores were immediately sectioned in 10-cm segments, which were placed in clean plastic containers for salinity and chlorophyll *a* (Chl *a*) measurements in the onboard laboratory after melting at 4°C in the dark. Ice temperature was measured in a separate companion core on site by embedding a stainless steel digital temperature probe in holes drilled to the center of the core at regular 5–10-cm intervals. The in situ temperature of sackhole brines was measured using the same instrument.

After determining the temperature of the brine in the hole, samples for O_2 determination were collected directly in 60-mL borosilicate glass bottles and were immediately fixed for Winkler titration. Samples for total alkalinity (A_T) were collected in a similar way, whereas aliquots for biological observations were fixed on the site as described below. Samples for the determination of total dissolved inorganic carbon (C_T) and its stable isotopic composition ($\delta^{13}C_T$) were collected in 20-mL plastic syringes and were dispensed through a cellulose nitrate filter (0.45 μm, Sartorius) into $HgCl_2$-poisoned 10-mL glass ampoules, which were stored flame-sealed under a nitrogen atmosphere for analysis in the home laboratory. The remaining brine was transported to the onboard laboratory into acid-washed polyethylene containers for immediate filtration through pre-combusted (550°C for 3 h) Whatman glass-fiber filters (GF/F, 0.7 μm) and subsequent sub-sampling for dissolved inorganic macronutrients (nitrate plus nitrite, phosphorus, and silicic acid), ammonium, and organic nitrogen (DON) into acid-washed 20–30-mL polypropylene bottles for subsequent analysis on location. The samples for the determination of dissolved organic carbon (DOC) were taken from the same filtrate; they were acidified with approximately 10 μL 85% H_3PO_4 and were stored at -20°C in pre-combusted (550°C for 3 h) 3-mL glass vials sealed with Teflon-lined septa for analysis in the home laboratory.

The surface seawater values presented here are means of discrete measurements in samples collected from 50-m water depth on six occasions in 12-liter bottles on the rosette sampler deployed with a conductivity-temperature-depth (CTD) instrument. Also included are seawater samples taken on three occasions at the floe by divers from near the ice–water interface, as well as samples of surface seawater collected on two occasions through ice holes during sackhole sampling.

Methods

The salinity was measured at laboratory temperature (17–22°C) using a portable conductivity meter (SEMAT Cond 315i/SET) with a WTW Tetracon 325 probe. The porosity of sea ice (V_b/V) was calculated from the measured bulk ice salinity and temperature as the percent fraction of unit volume of brine per unit volume of bulk ice using the equations in Cox and Weeks (1983), and in Leppäranta and Manninen (1988). The concentration of Chl *a* was determined on a Turner Designs TD-700 fluorometer following the method in Evans et al. (1987). Cell counting and identification of organisms (protists) were done with epifluorescence microscopy (Haas 1982), using a Leitz Dialux microscope equipped with epifluorescence light from a 50-W HBO mercury lamp. The samples were fixed upon sampling with ice-cold glutaraldehyde solution (1% final concentration) and were counted within 24 h and kept in the meantime at 4°C. Species identification with epifluorescence microscopy is usually limited, and many of the taxa are presented with the genus or group name only. Onboard analyses for the major dissolved inorganic nutrients, nitrate plus nitrite (hereafter, nitrate (NO_3^-)), dissolved inorganic phosphorus (DIP), and silicic acid, were done using standard colorimetric methodology (Grasshoff et al. 1983) as adapted for flow injection analysis (FIA) on a LACHAT Instruments Quick-Chem

8000 autoanalyzer (Hales et al. 2004). Dissolved ammonium (NH_4^+) was also determined onboard with the fluorimetric method of Holmes et al. (1999) using a HITACHI F2000 fluorescence spectrophotometer. DON was determined by subtraction of NO_3^- and NH_4^+ from the total dissolved nitrogen (TDN) analyzed by FIA on the LACHAT autoanalyzer using on-line peroxodisulfate oxidation coupled with ultraviolet radiation at pH 9.0 and 100°C (Kroon 1993). The agreement of duplicate low dissolved inorganic nitrogen samples (DIN = $[NO_3^-]$ + $[NH_4^+] < 1$ μmol kg^{-1}) analyzed on the daily calibration and separately by standard additions of nitrate and glycine standards was within 1–2 μmol kg^{-1} at the TDN concentration level of 8–20 μmol kg^{-1}. Further onboard measurements include O_2 by automated Winkler titration with photometric end-point detection, and A_T by potentiometric titration with 0.1 mol L^{-1} HCl (Titrisol) using a Metrohm system of automatic burette, pH meter, platinum temperature probe, Ag/AgCl reference electrode, and glass indicator electrode calibrated daily with NBS standards (for details, *see* Gleitz et al. 1995).

The DOC concentration was determined by high-temperature combustion on an MQ 1001 TOC Analyzer (Qian and Mopper 1996). Tested daily on the certified reference material of deep (700 m) Florida Strait seawater (Hansell Laboratory, University of Miami, Rosenstiel School of Marine and Atmospheric Science; batch 5 FS: 47–48 μmol L^{-1}), the method yielded 46 ± 3 μmol L^{-1} (n = 53), while the precision on duplicate brine samples was better than 10%. The C_T concentration and $\delta^{13}C_T$ were determined following in vacuo reaction with 85% H_3PO_4 and cryogenic CO_2 gas distillation using an in-line manometer and a EUROPA PDZ 20/20 mass spectrometer, respectively. The $\delta^{13}C_T$ measurements are reported relative to Vienna Pee Dee Belemnite (VPDB) as δ_{sample} = 1,000 [(R_{sample}/R_{VPDB}) − 1], where R = $^{13}C/^{12}C$. The pH at in situ temperature and salinity was computed from the A_T and C_T measurements and is reported on the seawater scale (pH_{SWS}), using the relevant temperature–salinity functions for acid-base equilibria in seawater appropriate for this pH scale and solving the system of the resulting equations with the Solver routine of Microsoft Excel. Specifically, the first and second stoichiometric dissociation constants of carbonic acid reported in Prieto and Millero (2002) were used ($pK_1^* = 5.84$ and $pK_2^* = 8.95$ at 25°C and a salinity of 35). The contributions of borate, DIP, silicic acid, and ammonium to A_T were taken into account, using the equations in Millero (1995). Details regarding the computations of the concentration of dissolved carbon dioxide (CO_2(aq)) in brine at equilibrium with air and the saturation state of the brine with respect to the anhydrous (calcite, aragonite, vaterite) and hydrated (ikaite) carbonate minerals at 1 atm as a function of temperature and salinity are given in Papadimitriou et al. (2004). The current atmospheric pCO_2 was set at 3.64×10^{-4} atm, equivalent to 374 ppmv measured during ISPOL (Hellmer et al. 2006). The concentration of O_2 in brine at equilibrium with air at 1 atm was computed as a function of temperature and salinity from the equation in Gacia and Gordon (1992). All the computations required extrapolation of the existing equations to the in situ values of temperature and salinity. Based on duplicate samples, the reproducibility of the O_2 measurements was better than 3% at 300–600 μmol kg^{-1}, whereas that of A_T measurements was better than 2% at 2,300–3,900 μmol eq kg^{-1}. Similarly, the reproducibility of duplicate C_T and $\delta^{13}C_T$ measurements was better than 2% at 3,000 μmol kg^{-1} and 0.2‰, respectively. The uncertainty in the A_T and C_T measurements translates into an uncertainty of 0.04 pH units and 1 μmol CO_2(aq) kg^{-1}, but the overall error of the computation can be as high as 0.07 pH units for pH_{SWS} and 30% for CO_2(aq) (Papadimitriou et al. 2004). The means of the observations at each sampling day were tested by analysis of variance in MINITAB for statistically significant differences (i.e., $p <$ 0.050) and are reported with ± 1σ.

Results

Bulk ice—The ice column in which the majority of the sampling (sackhole brine and ice cores) was conducted from day 336 to day 353 was mainly composed of columnar ice, with a 5–9-cm-thick layer of granular ice systematically observed between 17-cm and 25-cm depth below the surface. The freeboard in three ice core holes ranged from +4 cm to +9 cm, whereas there was no evidence (e.g., occurrence of superimposed ice layer at the ice surface) for the presence of snow meltwater during the period of this study. The bulk ice temperature ranged from −3.2°C to −1.7°C, with the lowest values (from −3.2°C to −2.7°C) recorded in the upper 60 cm of the ice column on first sampling (day 336, 01 December) and up to 1°C higher temperatures measured subsequently in the upper 140 cm of the ice column (Fig. 2a). As a result, the mean core temperature increased slightly but significantly ($p \leq 0.033$) from −2.5 ± 0.4°C (n = 18) on first sampling to −2.3 ± 0.2°C (n = 17) on days 346 and 353 of the year. The bulk ice salinity ranged from 3.0 to 8.4, with maximum values in the upper 60 cm and in the bottom 10 cm of the ice column (Fig. 2b). The salinity on first sampling was lower than subsequently measured within the bottom 80 cm of the ice column, but the mean core salinity did not exhibit a discernible temporal trend and had an overall mean of 5.2 ± 1.4 (n = 68). The ice porosity ranged from 6% to 21%, with a depth distribution in the ice column similar to that of bulk ice salinity (Fig. 2c). The mean ice porosity increased significantly (p = 0.024) from 9 ± 4% (n = 18) on day 336 to 12 ± 3% on day 346, whereas no further increase was observed by day 353 (12 ± 3%, n = 17). The increase in ice porosity was evident throughout the ice column and suggests an increase in ice permeability (Eicken 2003). The concentration of Chl *a* ranged from 0.3 μg L^{-1} to 138.0 μg L^{-1} and was highest (20–138 μg L^{-1}) in the bottom 3–7 cm of the ice column, with a secondary concentration peak of 5–19 μg L^{-1} at 50–60 cm below the ice surface (Fig. 2d).

The thickness of the ice and snow (150–180 cm and 30 cm, respectively) is relatively large for first-year sea ice in the Weddell Sea. This and the secondary peak in the concentration of Chl *a* in the upper part of the ice column (Fig. 2d) suggest an ice age longer than 1 yr. However, the

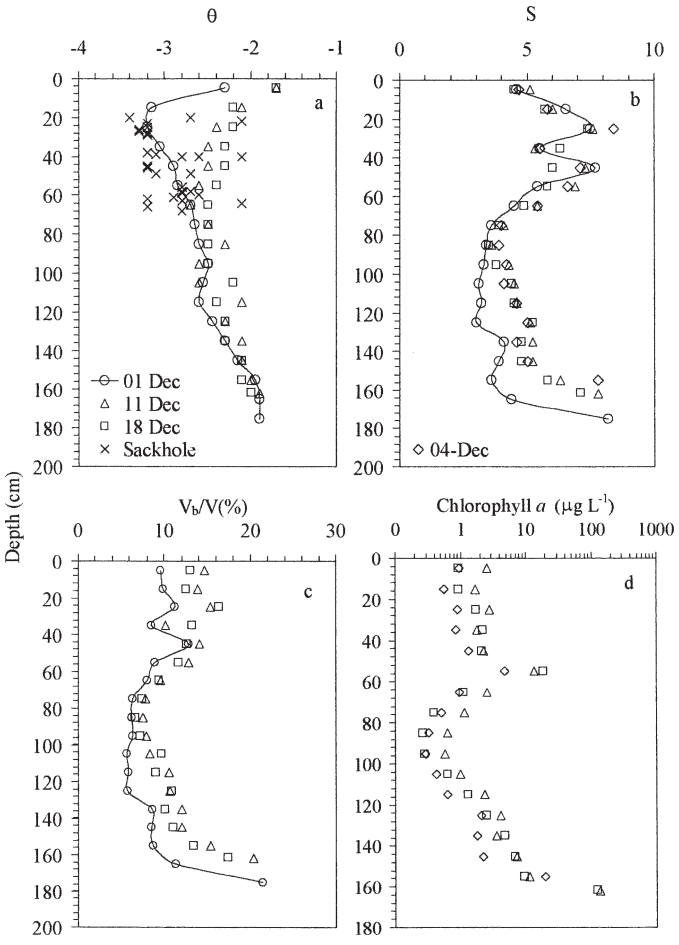

Fig. 2. Depth profiles of (a) temperature (θ), (b) salinity (S), (c) fractional brine volume (V_b/V), and (d) Chl *a* in ice cores taken on year days 336 (01 Dec), indicated by the linked symbols as the onset of this study, 339 (04 Dec), 346 (11 Dec), and 353 (18 Dec). Chl *a* in (d) is plotted on a logarithmic scale.

uniform columnar texture and its similarity to an adjacent sea ice band clearly identified by time series of satellite radar imagery as thick first-year ice originating from the Filchner-Ronne polynya (Hellmer et al. 2006) suggest that the sampled ice column was first-year ice. Consequently, we interpret the secondary peak in the concentration of Chl *a* in the upper part of the ice column as the result of an algal bloom under newly formed ice in the previous autumn in the Filchner-Ronne polynya.

Brine biological composition—Ciliates, dinoflagellates, and small aplasticid flagellated species were identified among the heterotrophic protist community of the first-year brines. The relative abundance of ciliates was highest in the initial samples taken on days 336 and 337, comprising more than 50% of the pool of individuals in the majority of the samples. Small flagellated species were dominant in numbers (i.e., >50% relative abundance) on day 340, and dinoflagellates dominated thereafter. No ciliates were observed in the second-year brine samples, which contained mainly dinoflagellates (95% relative abundance).

The autotrophic protist community of the first-year brines was dominated by flagellated prasinophytes and dinoflagellates throughout the study. No diatoms were found on day 336 but were observed in moderate abundance thereafter, which was always less than 50% of the pool of autotrophic individuals. The diatoms species found were identified as *Flagilariopsis* spp., *Chaetoceros*, and *Cylindrotheca* spp., with small and pale chloroplasts. The second-year brine samples contained small numbers of the above autotrophs, with diatoms comprising 35% of the pool. Overall, the distribution of dominant species likely reflects spatial variability rather than a temporal change given the small time frame of the study.

Chemical composition—Meaningful examination of the chemical composition of sea ice brines requires equivalent information for the parent water mass during sea ice formation. The heterogeneity of the ice floe notwithstanding, the characteristics of its parent water mass are not precisely known. As a convention, the chemical composition of the contemporaneous surface seawater will be used hereafter as a reference point. The ranges of the measured concentrations of A_T, and C_T in the brines are presented in Table 1, and those of NO_3^-, DIP, silicic acid, NH_4^+, DOC, and DON are presented in Table 2. In order to detect changes relative to surface seawater other than physical concentration of solutes during sea ice formation, the measured concentrations of the above solutes were normalized to a salinity of 34 (Gleitz et al. 1995) by

Table 1. Measured range of temperature (θ, in °C), salinity (S), total alkalinity (A_T), and total dissolved inorganic carbon (C_T), as well as mean ± 1σ of pH_{SWS}, O_2, salinity-normalized A_T ($[A_T]_S$), salinity-normalized C_T ($[C_T]_S$), and CO_2(aq) in brines from first- (days 336–352) and second-year sea ice (day 358). Solute concentrations are in μmol kg^{-1}, while A_T and $[A_T]_S$ are expressed in μmol eq kg^{-1}.

	Day of the year	*n**	θ	S	pH_{SWS}	O_2	A_T	$[A_T]_S$	C_T	$[C_T]_S$	CO_2(aq)
First-year ice	336	10	−3.4 to −3.2	60–63	8.57±0.08	319±118	4,178–4,369	2,362±25	3,234–3,526	1,859±71	10.7±2.8
	337	8	–3.4 to −3.1	59–63	8.54±0.06	280±67	4,102–4,620	2,362±59	3,206–3,551	1,882±48	11.4±1.9
	340	6	–2.9 to −2.8	53–55	8.62±0.03	466±68	3,751–3,865	2,392±22	2,900–3,073	1,875±32	7.7±0.8
	343	3	–2.7 to −2.6	51	8.71±0.06	454±51	3,435–3,563	2,338±54	2,636–2,677	1,774±20	5.4±1.0
	349	4	–2.8 to −2.7	44–45	8.66±0.03	514±66	3,147–3,215	2,434±31	2,443–2,558	1,927±45	5.6±0.6
	352	3	−2.1	40	8.79±0.05	602±2	2,690–2,807	2,358±43	2,091–2,112	1,790±16	3.5±0.5
Second-year ice	358	2	–3.1 to −2.8	57	8.76±0.01	432±3	3,469–3,556	2,107±34	2,508–2,585	1,527±31	4.4±0.1

* Number of samples from discrete sackhole cores.

Table 2. Measured range and mean $\pm 1\sigma$ of salinity-normalized solute concentrations ($[\ ]_S$), both in μmol kg^{-1}, in brines from first- (days 336–52) and second-year sea ice (day 358).

Day of the year	n*	NO_3^-	$[NO_3^-]_S$	NH_4^+	$[NH_4^+]_S$	DIP	$[DIP]_S$	Si	$[Si]_S$	DOC	$[DOC]_S$	DON	$[DON]_S$
336	10	0.4–1.0	0.4±0.1	0.8–2.4	0.66±0.24	1.31–2.05	0.93±0.12	66–80	40±3	211–343	160±20	14–19	9.1±1.0
337	7	0.5–1.0	0.4±0.1	0.4–1.2	0.40±0.15	0.82–2.03	0.78±0.24	53–66	34±2	202–342	163±25	11–17	8.1±1.3
340	6	0.3–2.1	0.4±0.4	0.1–0.6	0.18±0.10	0.47–0.64	0.34±0.04	38–58	31±5	134–180	95±10	8–9	5.0±0.4
343	3	1.5–3.1	1.4±0.5	0.4–0.5	0.30±0.07	0.49–0.65	0.37±0.05	40–50	29±3	165†	111†	12–13	8.3±0.1
349	4	0.1–0.3	0.1±0.1	0.3–0.4	0.30±0.04	0.36–0.49	0.31±0.05	44–47	35±1	112–182	104±24	16–26	14.3±3.5
352	3	0.2–0.4	0.3±0.1	0.6–0.8	0.60±0.07	0.36–0.43	0.34±0.04	4–13	8±4	214–242	183±24	16–19	14.8±1.1
358	2	0.6–1.0	0.5±0.1	0.8–1.0	0.55±0.11	0.35–0.41	0.23±0.02	38–39	28	216–231	134±6	9–10	5.6±0.3

* Number of samples from discrete sackholes.
† $n = 1$.

dividing by the degree of salt enrichment of the brines (*see* below), and are presented and discussed thus hereafter. The pH_{SWS} and the concentration of dissolved gases, O_2 and CO_2(aq), are more complex functions of salinity and temperature because of their direct dependence on the thermodynamic equilibria of gas exchange and acid–base reactions in the medium. As a result, these parameters cannot be normalized in a simple manner and are presented and discussed as measured.

The salinity (S) of the brines from first-year sea ice ranged from 40 to 63 and decreased over the course of the study (Table 1). Compared with the surface seawater salinity of $S_{SW} = 34$, the salt enrichment range of the brines was $E_S = S/S_{SW} = 1.17$–1.86. The temperature of the first-year brines ranged from -3.4°C to -2.1°C (Table 1), rising concurrently with the salinity decrease during the study. The brine collected from second-year sea ice was more saline and slightly colder than that from first-year sea ice at the time of sampling (Table 1). Overall, the difference of brine temperature from that of surface seawater (-1.85°C) was small.

The pH_{SWS} of the brines ranged from 8.42 to 8.83 and was higher than the surface seawater value by 0.25 to 0.66 units (Fig. 3a). The mean of the measurements obtained in each of the first 3 days of the study was significantly different from any of the daily means of the subsequent, more alkaline measurements (Table 1). The pH_{SWS} in the brine from second-year ice was also within the more alkaline range of measurements (Table 1).

The measured O_2 concentration ranged from 212 μmol kg^{-1} to 604 μmol kg^{-1} in the first-year brine (Fig. 3b). The samples collected on the first 2 days yielded significantly lower mean O_2 concentrations than subsequent samples (Table 1). The majority ($n = 11$) of the initial samples were undersaturated with respect to equilibrium with air, the rest ($n = 8$) being at or above the air saturation concentration (Fig. 3b). All subsequent first-year brine samples were well above the air saturation value at all times (Fig. 3b). The O_2 concentration in the second-year brine was also above air saturation (Fig. 3b). For comparison, the O_2 concentration in surface seawater (Fig. 3b) was below the air saturation value ($[O_2]_{sat} = 369$ μmol kg^{-1} at -1.85°C and S = 34).

The salinity-normalized A_T ($[A_T]_S$) in the first-year brine exhibited random variability around the mean surface seawater A_T (Fig. 4a). The mean of the observations obtained on day 349 was significantly different from that on any other day (Table 1). On this occasion, as well as on

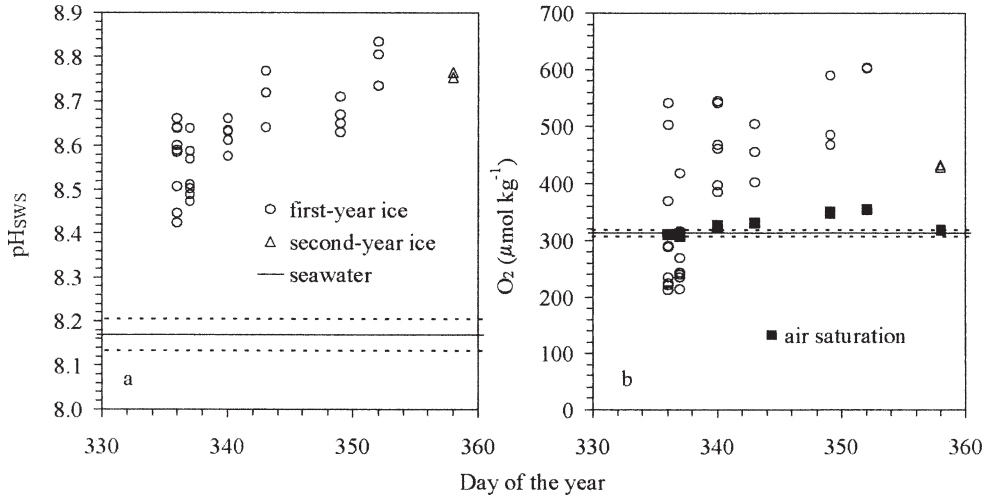

Fig. 3. (a) In situ pH_{SWS} (seawater scale) and (b) dissolved oxygen. The dotted lines indicate $\pm 1\sigma$ of the mean value in surface seawater.

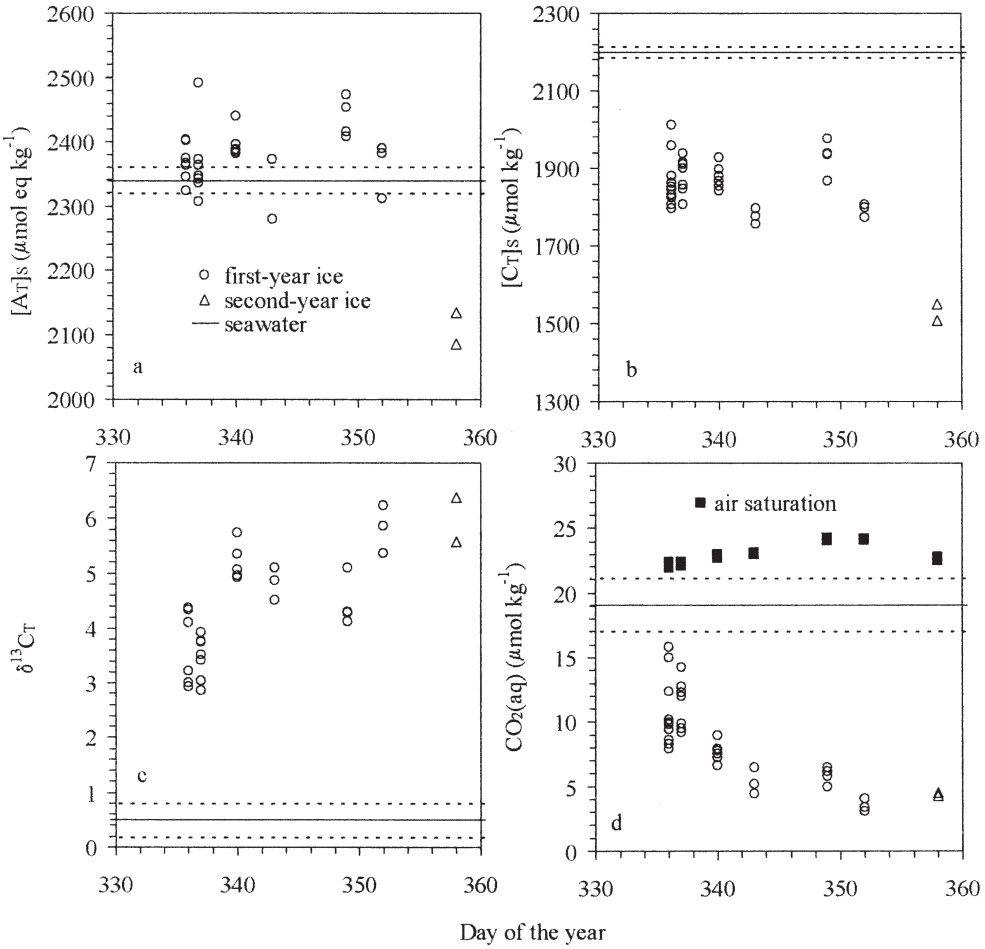

Fig. 4. (a) Salinity-normalized total alkalinity and (b) total dissolved inorganic carbon. (c) The stable isotopic composition of total dissolved inorganic carbon and (d) in situ concentration of dissolved carbon dioxide. The dotted lines are as in Fig. 2.

day 340, the mean $[A_T]_S$ in the brine was also significantly different from the mean surface seawater A_T, indicating excess $[A_T]_S$ by up to 150 μmol eq kg^{-1} (Fig. 4a). The brine obtained from second-year ice exhibited the lowest $[A_T]_S$ observed in this study (Table 1), significantly different from both first-year brine observations and the mean seawater A_T, indicating a deficit of approximately 200–250 μmol eq kg^{-1} (Fig. 4a). The salinity-normalized C_T ($[C_T]_S$) in the first-year brine deviated from the mean surface seawater concentration on all occasions, being always lower and, thus, exhibiting a relative deficit of 190–450 μmol kg^{-1} (Fig. 4b). This suggests a consistent net loss of inorganic carbon from the medium. A significantly lower mean $[C_T]_S$ was observed on days 343 and 352 than on any other sampling day (Table 1), indicating a higher $[C_T]_S$ deficit in the brine relative to surface seawater on these two occasions. The $[C_T]_S$ in the brine from second-year ice was the lowest observed in this study, with a significantly different mean concentration from those in both first-year brine (Table 1) and surface seawater, indicating a $[C_T]_S$ deficit of 650–700 μmol kg^{-1}. The measured $\delta^{13}C_T$ ranged from +2.9‰ to +6.4‰, exhibiting a large isotopic enrichment in the brine relative to the surface seawater value (Fig. 4c). A significant temporal shift toward greater ^{13}C enrichment by approximately +1.5 ± 0.8‰ on average was apparent in the first-year brine by comparison of the initial (days 336 and 337, $\delta^{13}C_T$ = +3.6 ± 0.5‰, n = 14) with the subsequent samples (days 340–352, $\delta^{13}C_T$ = +5.1 ± 0.6‰, n = 16).

The concentration of CO_2(aq) ranged from 3.1 μmol kg^{-1} to 15.9 μmol kg^{-1} and was less than the concentration calculated for equilibrium of brine with air at the in situ range of temperature and salinity conditions (Fig. 4d). The CO_2(aq) concentration exhibited changes during the course of the study from the significantly elevated mean concentrations in the initial samples on days 336 and 337 to progressively lower mean concentrations thereafter (Table 1). All brine samples were supersaturated (stoichiometric saturation index Ω = 1) with respect to the anhydrous $CaCO_3$ minerals calcite, aragonite, and vaterite, with average ($\pm 1\sigma$) indices of $\Omega_{calcite}$ = 12.2 ± 1.4, $\Omega_{aragonite}$ = 7.3 ± 0.8, $\Omega_{vaterite}$ = 2.7 ± 0.3 (n = 35). In contrast, all brine samples were below saturation with respect to ikaite, with an average Ω_{ikaite} = 0.8 ± 0.1 (n = 35). In comparison, the saturation index of surface seawater was less than that

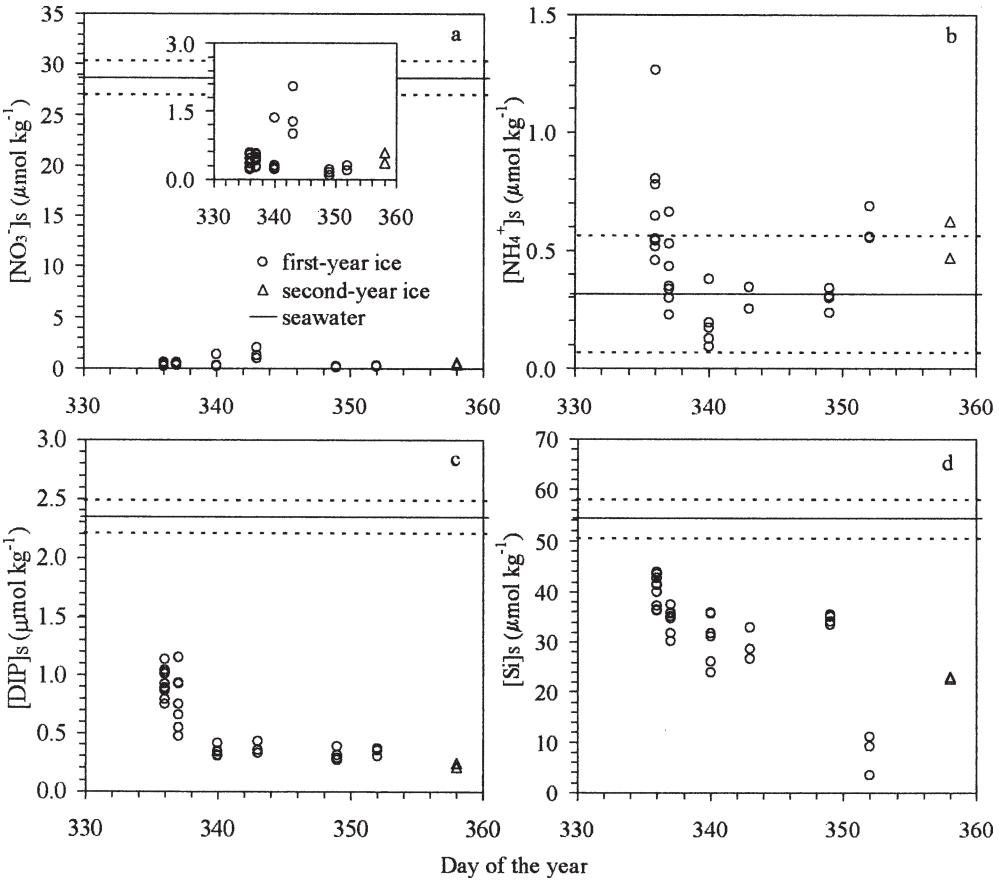

Fig. 5. The salinity-normalized concentration of dissolved inorganic nutrients (a) nitrate, (b) ammonium, (c) phosphorus, and (d) silicic acid. The dotted lines are as in Fig. 2.

in the brines by a factor of four, indicating supersaturation with respect to calcite and aragonite but undersaturation with respect to vaterite and ikaite.

While significant differences were observed for O_2, pH_{SWS}, $\delta^{13}C_T$, and $CO_2(aq)$ between the first 2 and subsequent sampling days, this was not so for the dissolved inorganic and organic components presented below, except for DIP. The salinity-normalized concentration of nitrate ($[NO_3^-]_S$) was always severely reduced in the brine from both the first- and second-year ice by comparison with the concentration in surface seawater (Fig. 5a). In the first-year brine, the mean $[NO_3^-]_S$ on day 343 was significantly higher than that on any other sampling occasion (Table 2). The salinity-normalized NH_4^+ ($[NH_4^+]_S$) in brines from both the first- and second-year ice was randomly distributed around the mean surface seawater concentration, except for a relative enrichment by a factor of 2–3 in individual first-year brine samples obtained on day 336 (Fig. 5b). The lowest $[NH_4^+]_S$ was observed in first-year ice on day 340, with a significantly different mean concentration from that in preceding and subsequent sampling occasions (Table 2). The salinity-normalized DIP ($[DIP]_S$, Fig. 5c) and silicic acid ($[Si]_S$, Fig. 5d) were reduced in the brine from both the first- and second-year ice relative to the composition of surface seawater. The mean $[DIP]_S$ observed in the first 2 sampling days (days 336 and 337) was significantly higher than the mean concentrations obtained thereafter (Table 2). The mean $[DIP]_S$ in the brine from second-year ice (Table 2) was significantly lower than that obtained from first-year ice. The highest and lowest mean $[Si]_S$ observed on the first (day 336) and last (day 352) sampling occasions in first-year sea ice, respectively, were significantly different from all other mean $[Si]_S$ observed in between (Table 2). The mean $[Si]_S$ in the brine from second-year ice (Table 2) was significantly lower than that in first-year ice except for the concentration minimum on day 352.

Both DOC and DON were elevated in the brine by comparison of their salinity-normalized concentrations, $[DOC]_S$ and $[DON]_S$, respectively, with surface seawater concentrations (Fig. 6). In the first-year brine, the mean $[DOC]_S$ was significantly higher on the first 2 (days 336 and 337) and the final (day 352) sampling days, with lower concentrations in between (Table 2). Similar differences in concentration were apparent and significant in the $[DON]_S$, with a sharper and significant minimum on day 340 (Table 2). The majority of the measured [DOC] and [DON] were positively correlated ($r = 0.821$, $p < 0.001$, $n = 30$), and the slope of the linear regression was equivalent to a mean ($\pm 1\sigma$) C:N = 19.0 ± 4.2 for the dissolved organic matter pool in the brines. The measurements obtained on day 349 were offset to the above trend, having a mean ($\pm 1\sigma$) C:N = 7.3 ± 0.4 ($n = 4$), as well as one of the measurements obtained on day 352, which yielded a C:N = 10.0.

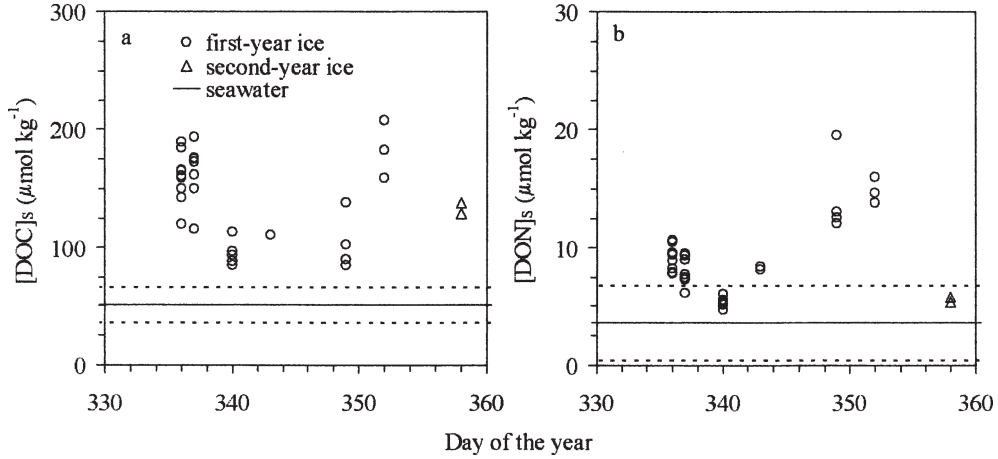

Fig. 6. The salinity-normalized concentration of (a) dissolved organic carbon, and (b) dissolved organic nitrogen. The dotted lines are as in Fig. 2.

Discussion

Brine origin—A marked characteristic of the current measurements in brine is the considerable variability observed on each sampling day. This was pronounced during the first 2 days of sampling (days 336 and 337) for most parameters, but sampling intensity was also maximal on these occasions. Analytical precision contributed only a small proportion to the observed variability. During the course of the study period, the first-year brine samples were removed from an area representing no greater than 6 m^2 of the floe. The above indicate a very high degree of spatial variability in biogeochemical parameters in natural first-year sea ice. The provenance of sackhole brine from within the ice column is difficult to assess. Brine is concentrated in pockets among ice crystals throughout the ice column in first-year ice. Brine inclusions vary in size and shape directly with ice porosity (brine volume), becoming larger and more elongated as ice porosity and temperature rise and with it their connectivity and the connectivity of different parts of the ice column (Perovich and Gow 1996). Small scale connectivity is established at ice porosities above 5–7% (Cox and Weeks 1975; Golden et al. 1998). Both ice temperature and porosity increased during the present study but not uniformly with depth in the ice (Fig. 2). Crucially for brine origin, there was a sustained ice porosity minimum of 6–10% within the 60–100-cm layer throughout the observation period, i.e., in the region of the threshold of small scale connectivity between the upper and bottom layers of the ice column. Direct comparison of the sackhole depth and brine temperature with the ice temperature depth profiles indicates that, in all cases but the last sackhole sampling (day 352), when brine temperatures were less than −2.5°C (Table 1), the samples must have originated in the upper 60–80 cm of the ice column, which exhibited temperatures less than −2.5°C (Fig. 2a).

The effect of physical processes on the composition of sea ice brine—Despite the large spatial variability in the composition of brine, differences were discernible between sampling days, which can be summarized as a shift toward higher pH_{SWS}, O_2, and $\delta^{13}C_T$, as well as lower DIP and CO_2(aq) in the latter half of the study period. The ionic composition of sea ice brine is controlled by physical, biological, and chemical processes. Physical processes include brine drainage by gravity and, when warming occurs, by its downward displacement by snow and ice meltwater advancing from the ice surface. Brine dilution with ice meltwater can also occur during the warming phase, when the meltwater is entrained within the ice column. Brine drainage ultimately results in the desalination of the ice, but reduction of bulk ice salinity was not evident in its depth profiles during the study period (Fig. 2b). On the other hand, the steady decrease in brine salinity (Table 1) indicates dilution by entrained ice meltwater as the temperature increased in the upper part of the ice column (Fig. 2a). The contribution of dilution to the most systematic compositional changes noted above was evaluated in a closed system, assuming the ice meltwater to be ion- and gas-free. Solute concentration in the brine was then calculated as $[(C_iS_b)/S_i]$, where C_i and S_i are the solute concentration and salinity, respectively, of the parent brine, from which the subsequent, less-saline brine of salinity S_b originated. The salinity and temperature of the diluted brine were set to co-vary as in their functional relationship in sea ice reported in Eicken (2003). The pH_{SWS} and CO_2(aq) were calculated from the predicted C_T and A_T of the diluted brine by solving the set of thermodynamic equations outlined earlier. The initial conditions for the parent brine were set at the maximum and minimum measurements obtained on first sampling (day 336). The large variability of these measurements, however, does not allow precise assessment of the subsequent changes as a function of the extent of brine dilution. In other words, the concept of a parent brine of singular chemical composition is an oversimplification for a medium as compositionally fragmented and heterogeneous as sea ice, especially at low porosity and low temperature. This uncertainty notwithstanding, model predictions show that the change caused by dilution in the pH_{SWS} and CO_2(aq) of a closed sea ice brine system resembles the observed temporal shift (Fig. 7a,b). The predicted dilution trend for

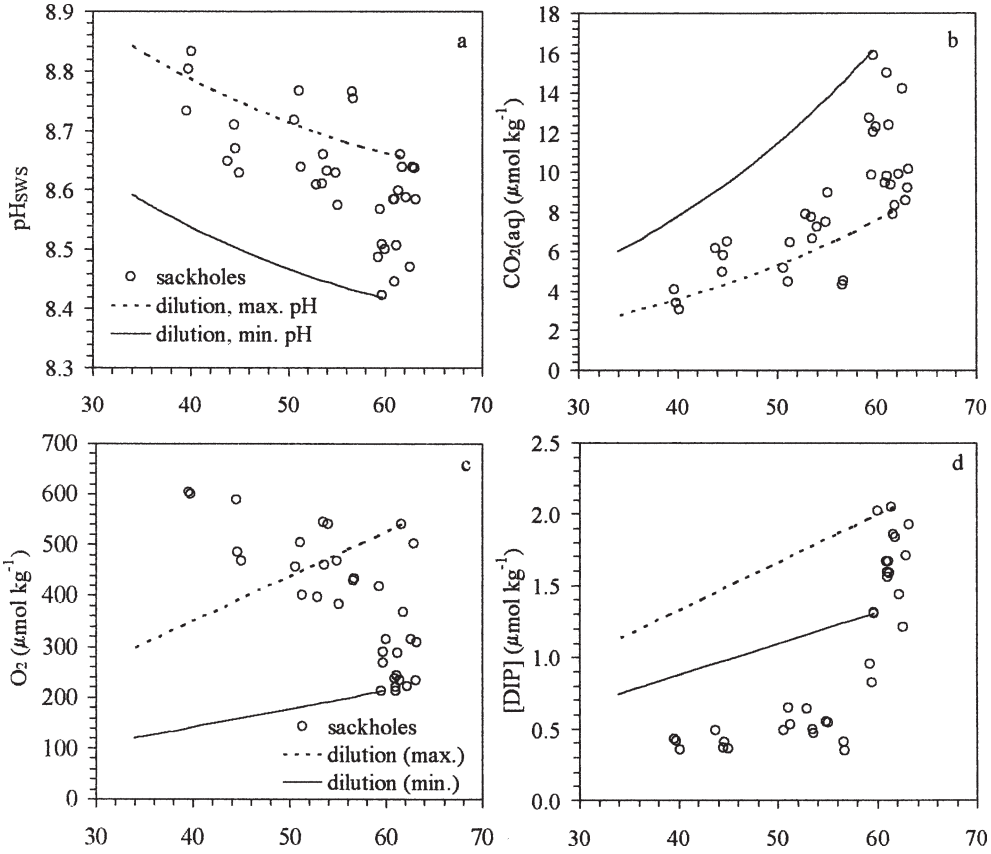

Fig. 7. (a) In situ pH_{SWS}, (b) dissolved carbon dioxide, (c) dissolved oxygen, and (d) measured dissolved inorganic phosphorus as a function of salinity in sackhole brines from first-year sea ice, with model trends predicted for dilution by entrained ice meltwater (*see* text for details).

O_2 is the opposite of that observed, suggesting accumulation in solution superimposed on the dilution effect (Fig. 7c). Lastly, the model predicts the decline in DIP, but an additional sink is clearly required for this solute (Fig. 7d), whereas dilution is not expected to have an effect on the stable carbon isotope ratio of C_T.

It is evident from the above that dilution by ice meltwater in a closed system cannot account collectively for every compositional change observed in the brine samples and its full extent. Next, the role of biological activity to the observed changes is assessed; first described for a large expanse of the Weddell Sea during austral summer and autumn in Gleitz et al. (1995), it is reiterated here for a single ice floe.

Biological activity—Primary productivity within sea ice in the Southern Ocean begins during its maximal extent in late austral spring (November), when the photoperiod and solar elevation increase, and peaks during sea ice decay in the summer (December–January), decreasing thereafter to slow rates until the early stages of new sea ice formation in autumn (April) (Arrigo et al. 1997). Production from the internal autotrophic community modifies distinctly the chemical composition of enclosed brines in sea ice (Gleitz et al. 1995). The degree of modification will depend upon the extent of solute exchange possible with the surface seawater, which is a function of ice porosity and snow cover that regulates freeboard. The significant reduction of the concentration of nitrate, DIP, and silicic acid; an increase of pH up to 10 and O_2 concentrations to well above air saturation; a decrease of C_T and CO_2(aq); and isotopic enrichment of the C_T pool due to the kinetically faster uptake of ^{12}C than ^{13}C during biological assimilation of inorganic carbon (Fogel and Cifuentes 1993) comprise the combined effect of primary production on the chemical composition of partially or fully isolated media and have been observed in field studies of internal and interfacial sea ice habitats (Gleitz et al. 1995; Kennedy et al. 2002; Kattner et al. 2004). These changes were evident in the current brine samples relative to the chemical composition of the surface seawater and in situ dissolved gas saturation estimates (Figs. 2–5), suggesting that the composition of the brine reflected mostly the imprint of primary productivity, but to a variable degree.

The drawdown of silicic acid (Fig. 5d) indicates uptake by the resident diatom population. The depth profiles of Chl *a*, taken as a proxy for the distribution of the autotrophic biomass in the ice column, suggest two potential loci of internal primary production in the first-year sea ice, in the bottom-most layer near the ice–water interface, and in the 50–60-cm layer below the ice surface (Fig. 2d). Considering that the brines likely originated in

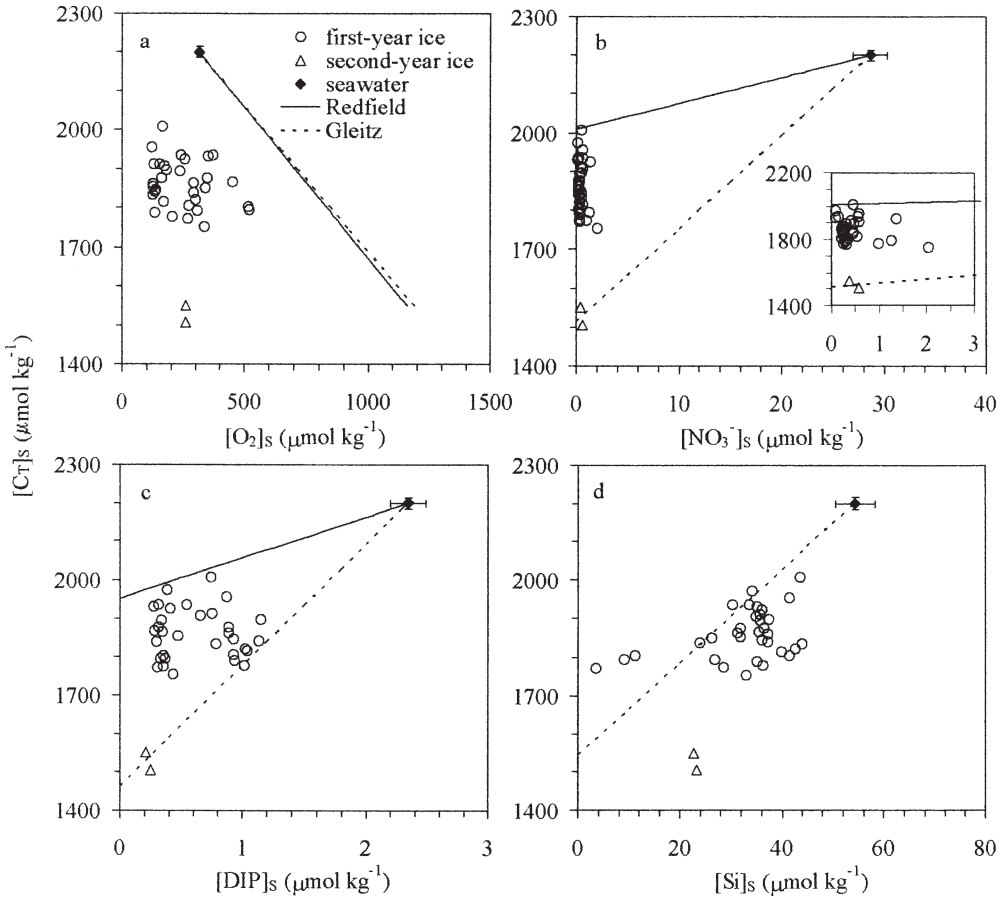

Fig. 8. Total dissolved inorganic carbon (C_T) as a function of (a) O_2, (b) nitrate plus nitrite (NO_3^-), (c) dissolved inorganic phosphorus (DIP), and (d) silicic acid (Si). All observations were normalized to a salinity of 34.

the upper and coldest part of the ice column (Fig. 2a), the collective compositional change relative to the composition of surface seawater should reflect the activity of organisms associated with the sub-surface peak in Chl *a*. The modification could have occurred before the study, e.g., during sea ice formation in the previous austral autumn, during the study period, or both. Some of the temporally distinct compositional changes appear to have occurred in the course of the study, either superimposed on (O_2, DIP), or regardless of ($\delta^{13}C_T$) the physical dilution effect during ice warming (Fig. 7). However, the considerable spatial variability of brine composition, especially during the early and colder sampling stage, does not allow a firm conclusion about the intensity of the internal biological productivity at the time of the study.

The elevated DOC and DON concentrations recorded in this study (Table 2), although low by comparison with measurements in Antarctic sea ice in other seasons (Thomas et al. 2001*a*), indicate substrate availability for production by heterotrophic microorganisms within the ice. Organic nitrogen metabolism leads to ammonium regeneration. Ammonium accumulation to high concentrations of up to 10–15 μmol kg^{-1} has been a feature of biologically productive sea ice habitats (Arrigo et al. 1995; Gleitz et al. 1995; Kattner et al. 2004) but was not evident in the current study (Table 2; Fig. 5b). The two major components of the dissolved inorganic nitrogen pool, nitrate and ammonium, were present at comparable low concentrations of mostly less than 1 μmol kg^{-1} throughout the study (Table 2), such that 80–90% of the total dissolved nitrogen pool was present as DON. This contrasts with the composition of sea ice later in austral summer, when high concentrations of inorganic nutrients have been measured, even at high rates of primary production, reflecting re-supply of nutrients from surface seawater, elevated rates of remineralization, or both (Thomas et al. 1998; Thomas et al. 2001*b*). Although the pool of inorganic macronutrients was not completely exhausted, the measured distribution of biologically available nitrogen between the inorganic and organic pools suggests that autotrophic inorganic nitrogen metabolism in the interior of the floe was likely constrained by the rate of heterotrophic DON remineralization at the time of the study.

There was no clear relationship between the salinity-normalized concentrations of C_T and the rest of the major inorganic nutrients (Fig. 8). The drawdown of silicic acid at a given $[C_T]_S$ deficit (Fig. 8d) was mostly less than predicted from the C to Si ratio reported for sea ice in Gleitz et al. (1995). When compared with the drawdown of nitrate and DIP in the brine, the range of the $[C_T]_S$ deficit

suggests an extremely variable stoichiometric uptake ratio of inorganic carbon to inorganic nitrogen and phosphorus (Fig. 8b,c). The current observations were nevertheless bracketed in both cases by the classic Redfield ratios, C : N = 6.625 and C : P = 106, as well as those based on the field observations of Gleitz et al. (1995), i.e., $[C_T]_S : [NO_3^-]_S$ = 24.0 and $[C_T]_S : [DIP]_S$ = 314.5. The drawdown of nitrate appears to be uniformly almost complete, i.e., equivalent to 93–100% of the concentration in surface seawater. The magnitude of the DIP drawdown, on the other hand, varied between 50% and 90% of the surface seawater concentration. For the observed nitrate drawdown, Redfield stoichiometry (N : P = 16) would give rise to a 76% drawdown of DIP, whereas N : P = 13.1, which can be calculated from the stoichiometric relationships in Gleitz et al. (1995), would extend the equivalent DIP drawdown to 93%. By comparison, the lower part (minimum) of the observed range in the $[DIP]_S$ deficit suggests an excess DIP relative to nitrate in the brine regardless of stoichiometric constraints, which is associated with the elevated DIP concentrations observed in the initial samples from first-year sea ice (days 336–337, Table 2). It is possible that faster remineralization of organically-bound phosphorus than organically-bound nitrogen and/or carbon within sea ice (Arrigo et al. 1995; Thomas et al. 1998; Thomas et al. 2001*b*) decoupled the DIP from both inorganic carbon and nitrogen dynamics in the brine.

The C_T pool in the brine was isotopically enriched (Fig. 4c) by comparison with the $\delta^{13}C_T$ in the world oceans (−0.5 to +1.5‰; Kroopnick 1985) and in productive sea ice habitats, such as platelet ice layers (+0.4 to +3.8‰; Thomas et al. 2001*b*), gap layers, and surface ponds (+0.2 to +3.0‰; Kennedy et al. 2002). Biological uptake of inorganic carbon fractionates strongly the stable carbon isotopes due to the faster fixation of $^{12}CO_2$ into biomass by the enzyme ribulose 1,5-biphosphate carboxylase oxygenase (Fogel and Cifuentes 1993). Thus, the produced organic carbon is isotopically depleted, whereas the residual C_T pool will become isotopically enriched depending on the openness of the system to solute exchange. The current $\delta^{13}C_T$ measurements approach values predicted for primary production in a closed sea ice system (Gleitz et al. 1996). The $\delta^{13}C_T$ was inversely proportional to $[C_T]_S$ (Fig. 9), hence a function of the magnitude of the C_T deficit in the brine, with a significant correlation in the more intensely sampled first-year ice (r = −0.564, n = 30, p = 0.001). Assuming a biological effect only, the amount and isotopic composition of the $[C_T]_S$ deficit in the brine will be equivalent to the amount and isotopic composition of the cumulative product of the process, i.e., particulate organic carbon (POC and $\delta^{13}C_{POC}$, respectively). For a given cumulative $\delta^{13}C_{POC}$, the concentration and isotopic composition of $[C_T]_S$ results from the modification of the concentration and isotopic composition of the parent water mass ($[C_T]_o$ and $\delta^{13}C_{To}$, respectively) by the amount of the $[C_T]_S$ deficit and its isotopic composition ($\delta^{13}C_{deficit}$), with $\delta^{13}C_{deficit} = \delta^{13}C_{POC}$, as the following isotopic mass balance demonstrates:

$$[C_T]_S \delta^{13}C_T = [C_T]_o \delta^{13}C_{To} - ([C_T]_o - [C_T]_S)\delta^{13}C_{POC} \quad (1)$$

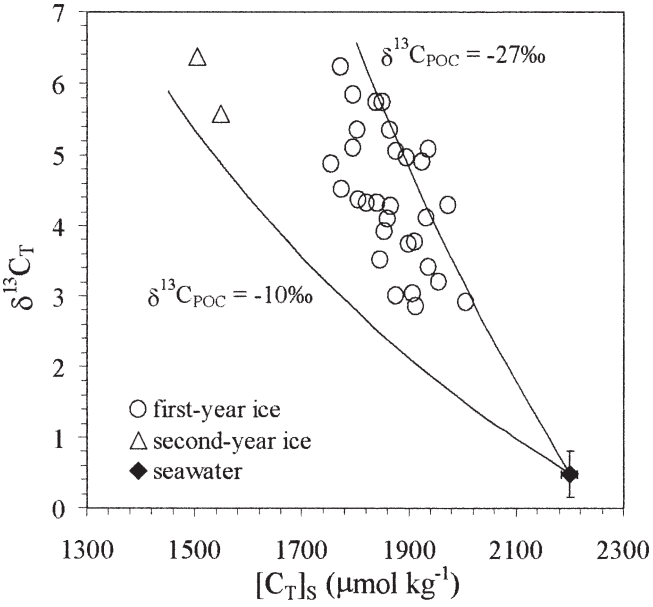

Fig. 9. The stable isotopic composition of total dissolved inorganic carbon ($\delta^{13}C_T$) as a function of the salinity-normalized C_T. The model curves are based on Eq. 1 (*see* text for details).

Division of both sides of the equation by $[C_T]_S$ and rearrangement gives $\delta^{13}C_T$ as a linear function of $[C_T]_S^{-1}$, with an intercept equivalent to $\delta^{13}C_{POC}$. The $\delta^{13}C_{POC}$ in sea ice has been reported to be very variable, ranging from −27‰ to −10‰ (McMinn et al. 1999; Thomas et al. 2001*b*; Kennedy et al. 2002). Setting this range of $\delta^{13}C_{POC}$ and using the mean surface seawater composition as $[C_T]_o$ and $\delta^{13}C_{To}$, trends in $\delta^{13}C_T$ can be predicted from the measured $[C_T]_S$, which encompass the current observations (Fig. 9). The simple model employed here for illustration demonstrates that the variability in the isotopic fractionation of the C_T pool in the brines was as large as that which would result from the reported $\delta^{13}C_{POC}$ in sea ice. The biological effect on stable carbon isotopes can be species-specific and depends on the concentration of CO_2 in the medium, among other parameters (Burkhardt et al. 1999). The variable $\delta^{13}C_{POC}$ implicit in the current $\delta^{13}C_T$ measurements can be associated with the variability seen in the CO_2(aq) concentration (Fig. 4d) and the outlined potential composition of the autotrophic protist community.

The deficit and isotopic enrichment of C_T (Fig. 9) are characteristic of primary production occurring in a closed or semi-closed system and would be expected to be associated with O_2 accumulation and, hence, supersaturation in solution. Although this was the prevailing condition in the course of this study, 60% of the initial observations (days 336 and 337) indicated O_2 undersaturation (Fig. 3d). Autotrophic production and oxygen-consuming, respiratory CO_2-yielding heterotrophic production within sea ice would be expected to couple the O_2 and C_T dynamics in a relationship shaped by the net stoichiometry of biological activity in the absence of further reactions, such as gas exchange. In contrast to the linear relationship between the salinity-normalized concentrations of O_2 ($[O_2]_S$) and $[C_T]_S$ described in Gleitz et al. (1995), the concentration changes

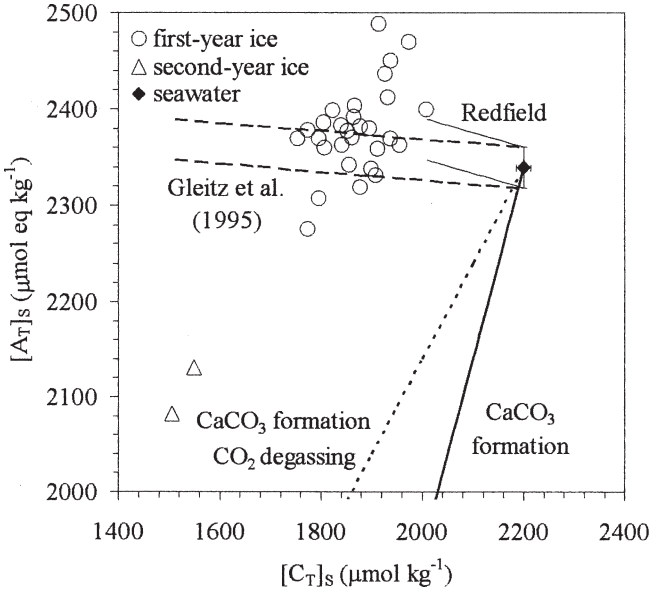

Fig. 10. Salinity-normalized total alkalinity ($[A_T]_S$) versus salinity-normalized total dissolved inorganic carbon ($[C_T]_S$). The parallel solid and dashed lines indicate concentration changes during photosynthetic nitrate uptake to exhaustion proceeding with a stoichiometry based on the Redfield C : N ratio and that reported in Gleitz et al. (1995), using the minimum and maximum $A_T \pm 1\sigma$ in surface seawater as initial concentration. The solid and dotted lines indicate concentration changes during $CaCO_3$ formation with and without CO_2 degassing.

seen here for these parameters (Fig. 8a) were independent from each other, with a weak correlation ($r = -0.215$, $p = 0.237$, $n = 32$). Further, regardless of the observed saturation state of the brine with respect to O_2 and for a given C_T deficit, the $[O_2]_S$ concentration was always less than predicted for the modification of the composition of surface seawater by biological activity proceeding at the Redfield $C : O_2$ stoichiometry (-0.77) or the similar $C : O_2$ of -0.74 reported in Gleitz et al. (1995) for austral summer and autumn (Fig. 8a). All current observations, therefore, appear offset in the direction of O_2 relative to theoretical stoichiometric trends. The above indicate that the biology-induced pairing of O_2 and C_T dynamics could be disrupted within sea ice, most likely by O_2 loss through degassing, as has been documented experimentally in the early stages of artificial ice formation (Killawee et al. 1998).

Primary production results in a small A_T increase, mostly through the uptake of nitrate (Lazar and Loya 1991), relative to the C_T decrease at a molar ratio equivalent to the N : C of the biological assimilation. The $[A_T]_S$ and $[C_T]_S$ from first-year ice were mostly consistent with a $\Delta A_T : \Delta C_T = -0.042$ based on the N : C reported for sea ice in Gleitz et al. (1995) (Fig. 10). The second-year brine samples, however, indicated concurrent reduction in $[A_T]_S$ and $[C_T]_S$ relative to surface seawater, which deviated from predictions for biological activity and are consistent with $CaCO_3$ formation (Fig. 10). Carbonate mineral formation reduces A_T in direct proportion to the decrease in C_T at a molar ratio of $\Delta A_T : \Delta C_T = 1$ when accompanied by degassing of the produced CO_2, or $\Delta A_T : \Delta C_T = 2$ when the produced CO_2 accumulates in solution (Lazar and Loya 1991).

It is apparent that there was no widespread precipitation of $CaCO_3$ in the first-year sea ice at the conditions of temperature (-3.4°C to -2.1°C) described in this work, even at the elevated anhydrous $CaCO_3$ supersaturation indices outlined earlier. Although very much lower than the experimental inhibitory DIP concentration of 5 μmol kg^{-1} or more (Bischoff et al. 1993), the presence of DIP in the brine (Fig. 5c) may still impede the precipitation of the anhydrous $CaCO_3$ minerals. Similarly, elevated DOC concentrations have been found to delay their formation (Chave and Suess 1970). Interference from the inorganic and organic matrix, therefore, could explain the high degree of supersaturation with respect to anhydrous $CaCO_3$ minerals consistently sustained in all of the current brine samples.

Little is known about the occurrence and behavior of the hydrated form of $CaCO_3$ (ikaite) in sea ice. Thermodynamic modeling of brine at sub-zero temperatures and at equilibrium with atmospheric CO_2 predicted the onset of ikaite formation at a temperature of -4.5°C in the absence of anhydrous $CaCO_3$ mineral formation (FREZCHEM model; Marion 2001). The current brine samples were undersaturated with respect to atmospheric CO_2 (Fig. 4d), presumably as a result of biological CO_2 uptake. The FREZCHEM model predicted ikaite formation in the absence of anhydrous $CaCO_3$ formation at progressively higher temperatures than -4.5°C when the CO_2(aq) concentration in the brine was lower than atmospheric equilibrium (unpubl. data). These conditions were not met in the first-year brine samples, but the model predicted ikaite precipitation at temperature and CO_2(aq) conditions similar to those observed in the second-year brine samples (Table 1). Carbonate mineral formation can also result in fractionation of the stable carbon isotopes. At isotopic equilibrium and 0°C, for example, calcite and aragonite are enriched in ^{13}C relative to CO_2(aq) (Romanek et al. 1992). By comparison with the faster biological processing of ^{12}C, $CaCO_3$ precipitation at isotopic equilibrium will have the opposite effect, thus moderating to some extent the biologically-mediated isotopic enrichment of the residual C_T pool. The isotopic enrichment was moderate for the extent of the $[C_T]_S$ deficit in the brine from second-year sea ice by comparison with the remainder of the data from first-year sea ice (Fig. 9), consistent with either a reduction in isotopic fractionation during biological uptake and/or the occurrence of $CaCO_3$ formation suggested by the $[A_T]_S$ and $[C_T]_S$ changes in this case (Fig. 10).

In summary, spatial variability within the sampling location marked the current observations, as well as signs of biological activity as primary production within sea ice. The latter signs were traced in the O_2 concentration as mostly exceeding air saturation, a pH increase by a maximum of approximately 0.6 units, the drawdown of all inorganic macronutrients to very low concentrations, and an isotopic enrichment of the C_T pool by approximately 6‰, all relative to the composition of surface oceanic water. However, there was no internal relationship evident among the macronutrients (including inorganic carbon) and O_2 as

would have been expected from stoichiometric constraints of their biological processing. This appears to be due to variable stoichiometry of the biological reaction and a pronounced O_2 loss from the brine. Prolonged degassing of autumnal hyperoxic brine during winter, when biological activity is at its seasonal minimum due to light limitation and extremely low temperature, can be expected to increase the divergence of O_2 from a biology-induced relationship with C_T in brine recovered early in the following summer. Carbonate mineral formation, a potentially contributing process with a comparatively large stoichiometric effect manifest in the A_T to C_T ratio, was not evident in the temperature (-3.4°C to -2.1°C) range of the brines recovered from first-year sea ice. Only the A_T and C_T changes in second-year ice were clearly commensurate with $CaCO_3$ formation, but generalizations about the occurrence and contribution of carbonate mineral formation to the total carbon sink within sea ice cannot be made on the current findings. A more direct approach to this process is clearly required, especially during austral winter, when sea ice brine is expected to provide the ideal physical–chemical environment for mineral formation with the development of the most saline and coldest conditions of the year with minimum biological activity.

References

Arrigo, K. R. 2003. Primary production in sea ice, p. 143–183. *In* D. N. Thomas and G. S. Dieckmann [eds.], Sea ice: An introduction to its physics, chemistry, biology and geology. Blackwell.

———, G. Dieckmann, M. Gosselin, D. H. Robinson, C. H. Fritsen, and C. W. Sullivan. 1995. High resolution study of the platelet ice ecosystem in McMurdo Sound, Antarctica: Biomass, nutrient, and production profiles within a dense microalgal bloom. Mar. Ecol. Prog. Ser. **127:** 255–268.

———, and D. N. Thomas. 2004. The importance of sea ice for the Southern Ocean ecosystem. Antarct. Sci. **16:** 471–486.

———, D. L. Worthen, M. P. Lizotte, P. Dixon, and G. Dieckmann. 1997. Primary production in Antarctic sea ice. Science **276:** 394–397.

Bischoff, J. L., J. A. Fitzpatrick, and R. J. Rosenbauer. 1993. The solubility and stabilization of ikaite ($CaCO_3 \cdot 6H_2O$) from 0° to 25°C: Environmental and paleoclimatic implications for thinolite tufa. J. Geol. **101:** 21–33.

Brierley, A. S., and D. N. Thomas. 2002. The ecology of Southern Ocean pack ice. Adv. Mar. Biol. **43:** 171–278.

Burkhardt, S., U. Riebesell, and I. Zondervan. 1999. Effects of growth rate, CO_2 limitation and cell size on the stable carbon isotope fractionation in marine phytoplankton. Geochim. Cosmochim. Acta **63:** 3729–3741.

Chave, K. E., and E. Suess. 1970. Calcium carbonate saturation in seawater: Effects of dissolved organic matter. Limnol. Oceanogr. **15:** 633–637.

Comiso, J. C. 2003. Large-scale characteristics and variability of the global sea ice cover, p. 112–142. *In* D. N. Thomas and G. S. Dieckmann [eds.], Sea ice: An introduction to its physics, chemistry, biology and geology. Blackwell.

Cox, G. F. N., and W. F. Weeks. 1975. Brine drainage and initial salt entrapment in sodium chloride ice. CRREL Research Report 345.

———, and ———. 1983. Equations for determining the gas and brine volumes in sea ice samples. J. Glaciol. **29:** 306–316.

Eicken, H. 2003. From the microscopic, to the macroscopic, to the regional scale: Growth, microstructure and properties of sea ice, p. 22–81. *In* D. N. Thomas and G. S. Dieckmann [eds.], Sea ice: An introduction to its physics, chemistry, biology and geology. Blackwell.

Emerson, S. 1975. Gas exchange rates in small Canadian Shield lakes. Limnol. Oceanogr. **20:** 754–761.

Evans, C. A., J. E. O'reilly, and J. P. Thomas. 1987. A handbook for the measurement of chlorophyll *a* and primary production. Biological investigations of marine Antarctic systems and stocks (BIOMASS). Texas A&M University.

Fogel, M. L., and L. A. Cifuentes. 1993. Isotope fractionation during primary production, p. 73–98. *In* M. H. Engel and S. A. Macko [eds.], Organic geochemistry: Principles and applications. Plenum Press.

Francois, R., and others. 1997. Contribution of Southern Ocean surface-water stratification to low atmospheric CO_2 concentrations during the last glacial period. Nature **389:** 929–935.

Gacia, H. E., and L. I. Gordon. 1992. Oxygen solubility in seawater: Better fitting equations. Limnol. Oceanogr. **37:** 1307–1312.

Gleitz, M., and D. N. Thomas. 1993. Variation in phytoplankton standing stock, chemical composition and physiology during sea-ice formation in the southeastern Weddell Sea, Antarctica. J. Exp. Mr. Biol. Ecol. **173:** 211–230.

———, H. Kukert, U. Riebesell, and G. S. Dieckmann. 1996. Carbon acquisition and growth of Antarctic sea ice diatoms in closed bottle incubations. Mar. Ecol. Prog. Ser. **135:** 169–177.

———, M. Rutgers van der Loeff, D. N. Thomas, G. S. Dieckmann, and F. J. Millero. 1995. Comparison of summer and winter inorganic carbon, oxygen and nutrient concentrations in Antarctic sea ice brines. Mar. Chem. **51:** 81–91.

Golden, K. M., S. F. Ackley, and V. I. Lytle. 1998. The percolation phase transition in sea ice. Science **282:** 2238–2241.

Grasshoff, K., M. Ehrhardt, and K. Kremling. 1983. Methods of seawater analysis. Verlag Chemie.

Haas, L. W. 1982. Improved epifluorescence microscopy for observing planktonic micro-organisms. Ann. Inst. Océanogr. Suppl. **58:** 261–266.

Hales, B., A. van Greer, and T. Takahashi. 2004. High-frequency measurements of seawater chemistry: Flow-injection analysis of macronutrients. Limnol. Oceanogr. Methods **2:** 91–101.

Hellmer, H. H., C. Haas, G. S. Dieckmann, and M. Schroder. 2006. Sea ice feedbacks observed in western Weddell Sea. Eos Trans. Am. Geophys. Union **87:** 173–184.

Holmes, R. M., A. Aminot, R. Kerouel, B. A. Hocker, and B. J. Peterson. 1999. A simple and precise method for measuring ammonium in marine and fresh water. Can. J. Fish. Aquat. Sci. **56:** 1801–1808.

Kattner, G., D. N. Thomas, C. Haas, H. Kennedy, and G. S. Dieckmann. 2004. Surface ice and gap layers in Antarctic sea ice: Highly productive habitats. Ecol. Progr. Ser. **277:** 1–12.

Kennedy, H., D. N. Thomas, G. Kattner, C. Haas, and G. S. Dieckmann. 2002. Particulate organic matter in Antarctic summer sea ice: concentration and stable isotopic composition. Mar. Ecol. Prog. Ser. **238:** 1–13.

Killawee, J. A., I. J. Fairchild, J. L. Tison, L. Janssens, and R. Lorrain. 1998. Segregation of solutes and gases in experimental freezing of dilute solutions: Implications for natural glacial systems. Geochim. Cosmochim. Acta **62:** 3637–3655.

KROON, H. 1993. Determination of nitrogen in water: Comparison of continuous flow method with on-line UV digestion with the original Kjedahl method. Anal. Chim. Acta **276:** 287–293.

KROOPNICK, P. M. 1985. The distribution of ^{13}C of ΣCO_2 in the world oceans. Deep-Sea Res. **32:** 57–84.

LAZAR, B., AND Y. LOYA. 1991. Bioerosion of coral reefs—A chemical approach. Limnol. Oceanogr. **36:** 377–383.

LEPPÄRANTA, M., AND T. MANNINEN. 1988. The brine and gas content of sea ice with attention to low salinities and high temperatures.Finnish Institute Marine Research Internal Report **88-2**. Helsinki.

MARION, G. M. 2001. Carbonate mineral solubility at low temperatures in the Na-K-Mg-Ca-H-Cl-SO_4-OH-HCO_3-CO_3-CO_2-H_2O system. Geochim. Cosmochim. Acta **65:** 1883–1896.

———, AND R. E. FARREN. 1999. Mineral solubilities in the Na-K-Mg-Ca-Cl-SO_4-H_2O system: A re-evaluation of the sulphate chemistry in the Spencer-Moller-Weare model. Geochim. Cosmochim. Acta **63:** 1305–1318.

MCMINN, A., J. SKERRATT, T. TRULL, C. ASHWORTH, AND M. LIZOTTE. 1999. Nutrient stress gradient in the bottom 5 cm of fast ice, McMurdo Sound, Antarctica. Polar Biol. **21:** 220–227.

MILLERO, F. J. 1995. Thermodynamics of the carbondioxide system in the oceans. Geochim. Cosmochim. Acta **59:** 661–677.

PAPADIMITRIOU, S., H. KENNEDY, G. KATTNER, G. S. DIECKMANN, AND D. N. THOMAS. 2004. Experimental evidence for carbonate precipitation and CO_2 degassing during sea ice formation. Geochim. Cosmochim. Acta **68:** 1749–1761.

PEROVICH, D. K., AND A. J. GOW. 1996. A quantitative description of sea ice inclusions. J. Geophys. Res. **101:** 18327–18343.

PRIETO, F. J. M., AND F. J. MILLERO. 2002. The values of pK_1 + pK_2 for the dissociation of carbonic acid in seawater. Geochim. Cosmochim. Acta **66:** 2529–2540.

RYSGAARD, S., R. N. GLUD, M. K. SEJR, J. BENDTSEN, AND P. B. CHRISTENSEN. 2007. Inorganic carbon transport during sea ice growth and decay: A carbon pump in polar seas. J. Geophys. Res. **112:** C03016, doi: 19.1029/2006JC003572.

QIAN, J., AND K. MOPPER. 1996. High performance high temperature combustion total organic carbon analyzer. Anal. Chem. **68:** 3090–3097.

ROMANEK, C. S., E. L. GROSSMAN, AND J. W. MORSE. 1992. Carbon isotopic fractionation in synthetic calcite and aragonite: Effects of temperature and precipitation rate. Geochim. Cosmochim. Acta **56:** 419–430.

STEPHENS, B. B., AND R. F. KEELING. 2000. The influence of Antarctic sea ice on glacial-interglacial CO_2 variations. Nature **404:** 171–174.

THOMAS, D. N., AND G. S. DIECKMANN. 2002. Antarctic sea ice—a habitat for extremophiles. Science **295:** 641–644.

———, R. ENGBRODT, V. GIANNELLI, G. KATTNER, H. KENNEDY, C. HAAS, AND G. S. DIECKMANN. 2001*a*. Dissolved organic matter in Antarctic sea ice. Ann. Glaciol. **33:** 297–303.

———, H. KENNEDY, G. KATTNER, D. GERDES, C. GOUGH, AND G. S. DIECKMANN. 2001*b*. Biogeochemistry of platelet ice: its influence on particle flux under fast ice in the Weddell Sea, Antarctica. Polar Biol. **24:** 486–496.

———, AND OTHERS. 1998. Biological soup within decaying summer sea ice in the Amudsen Sea, Antarctica. Antarctic Sea Ice Biological Processes, Interactions, and Variability, AGU Washington, Ant. Res. Ser. **73:** 161–171.

TISON, J. L., C. HAAS, M. M. GOWING, S. SLEEWAEGEN, AND A. BERNARD. 2002. Tank study of physico-chemical controls on gas content and composition during growth of young sea ice. J. Glaciol. **48:** 177–191.

WEISSENBERGER, J. 1992. The environmental conditions in the brine channels of Antarctic sea ice. Reports on Polar Research **111:** 1–159.

Received: 7 July 2006
Accepted: 5 April 2007
Amended: 15 May 2007